DID THE CESSATION OF CONVECTION IN MERCURY'S MANTLE ALLOW FOR AN INCREASE IN THE RATE OF HEAT LOSS FROM ITS CORE? J. M. Guerrero[1], J. P. Lowman[2], & P. J. Tackley[3], [1]Department of Physics, University of Toronto, Toronto M5S 1A7, Canada (joshua.guerrero@mail.utoronto.ca), [2]Department of Physical and Environmental Sciences, University of Toronto Scarborough, Toronto M1C 1A4, Canada., [3]Department of Earth Sciences, ETH-Zurich, Sonneggstrasse 5, 8092 Zurich, Switzerland.

Introduction: Mercury's mysterious magnetic field is hydrodynamic in origin [e.g., 1,2,3,4]. Thus, for the generation of a dynamo, ohmic heat dissipation requires that a minimum amount of heat must be adsorbed by Mercury's mantle from its (at least) partially molten core. Mercury's thin mantle and small size combine to allow the possibility that as its mantle cools over time, the dominant heat transfer mechanism from core to surface may change from convection to conduction, affecting how much heat can be extracted from the core throughout its evolution [5,6,7].

In numerical models post-MESSENGER, Michel et al., (2013) simulate Mercurian mantle convection using 2-D axisymmetric spherical segments. They find that mantle convection can persist to present-day as long as the mantle is thicker than 300 km. Tosi et al., (2013) have investigated the thermochemical evolution of Mercury's interior using 2-D cylindrical and 3-D spherical shell geometries and find that for most of their models, mantle convection ceases after 3-4 Gyr.

In this work, we model the evolution of Mercury's thin spherical shell geometry mantle over five billion years of evolution to determine whether high heat flows at the core-mantle boundary (consistent with a magnetic dynamo) are possible at present-day. Secular cooling featuring different initial internal heat production rates is examined. For different parameters we determine the evolving modes of heat transfer in the mantle and rate of heat flow at the core-mantle boundary at present-day.

Methods: Thermally driven convection in a Boussinesq fluid with infinite Prandtl number is modeled in a fully three-dimensional spherical shell geometry. A hybrid finite-difference/finite-volume code, StagYY, solves the governing equations, using a parallelized multigrid method [8,9]. Our calculations emulate secular cooling of a Mercurian mantle. The surface and core-mantle boundary are modeled as free-slip in each calculation and are isothermally fixed to $T = T_{surf}$ and $T = T_{cmb}(t)$. The core-mantle boundary temperature is evolved by adjusting the change in energy of the core given the basal heat flow from the mantle.

Our initial condition emulates a well mixed post-magma ocean characterized by a conducting lid overlying an interior with a temperature profile specified by the solidus curve of peridotite. We employ a core radius to outer shell radius ratio of 0.83 (implying a mantle thickness of 420 km if R_{surf} = 2440 km [10]) and feature four decaying internal heating rates, H, spanning from 10 to 40 pW/kg at $t = 0$ Gyr.

An Arrhenius rheology law is implemented, with an activation energy of 300 kJ/mol and a reference viscosity of 10^{21} Pa.s at a temperature of 1600 K. We consider calculations with an evolving viscosity contrast $\Delta\eta_{var} = \eta(T_{clip})/\eta(T_{cmb})$ where any material colder than T_{clip} is assigned to the maximum viscosity $\eta(T_{clip})$. The viscosity contrast is 10^{10} initially and decreases over time as the core-mantle boundary cools.

We consider a mantle with poorly constrained iron content and propose that the thermal conductivity (and hence the thermal diffusivity, κ) may be larger than for the Earth's mantle. Specifically, we adopt homogeneous values of κ for the Mercurian mantle between 1 mm^2/s and 3 mm^2/s for different suites of calculations.

We consider a calculation compatible with a present-day Mercurian dynamo if at 4.5 Gyr of evolution the CMB temperature is in excess of 1325 K (i.e., the core temperature is above the solidus temperature) and the CMB heat flux is greater than or equal to 12 mW/m^2 [11].

Results: To distill the effect of initial internal heating rate a thermal diffusivity of κ = 1 mm^2/s is first employed. Next, emulating the potential effect of metal content on mantle properties we examine the sensitivity of the results by increasing the thermal diffusivity as an analogue to thermal conductivity. Finally, the effect of rheology (i.e., an alternative mantle chemistry) is investigated, by varying the reference viscosity for a subset of the dynamo compatible cases.

Figure 1 shows the effect of initial internal heating rate on the evolution of the Mercurian mantle. For each calculation we find that heat flux is in excess of 19 mW/m^2 within the first 300 Myr of evolution but well below 12 mW/m^2 at present-day. As the systems we model cool, we find that the mean core heat flux reaches a temporal local minimum when the mantle transitions from a convective to a conductive regime and then subsequently climbs before decreasing. The transition to conduction is delayed with increased heating rate but the maximum mean heat flux from the core is strongly dependent on the mantle internal heating rate and is always greater than the heat flux observed at the cessation of the stagnant-lid convection. Delay time for reaching the maximum heat flux attained following the local minimum can exceed 1 Gyr.

For the sensitivity of core heat flux to thermal diffusivity we find that the transition to conduction occurs earlier with an increased κ. Finally, we consider cases with an initially more vigorously convecting mantle and find that a reduced reference viscosity (by a factor of 5) marginally reduces the basal heat flux at present day. For the highest χ tested, the basal heat flux falls below 12 mW/m^2 as a result of viscosity reduction disqualifying the case from compatibility with a Mercurian dynamo.

In Figure 2 we summarize our results in χ-κ space and find that for a narrow range of parameters (e.g., κ > 1 mm^2/s and $\chi \leq$ 30 pW/kg) conductive cooling of the mantle may result in a core heat flux that is in excess of 12 mW/m^2 at present-day (green symbols).

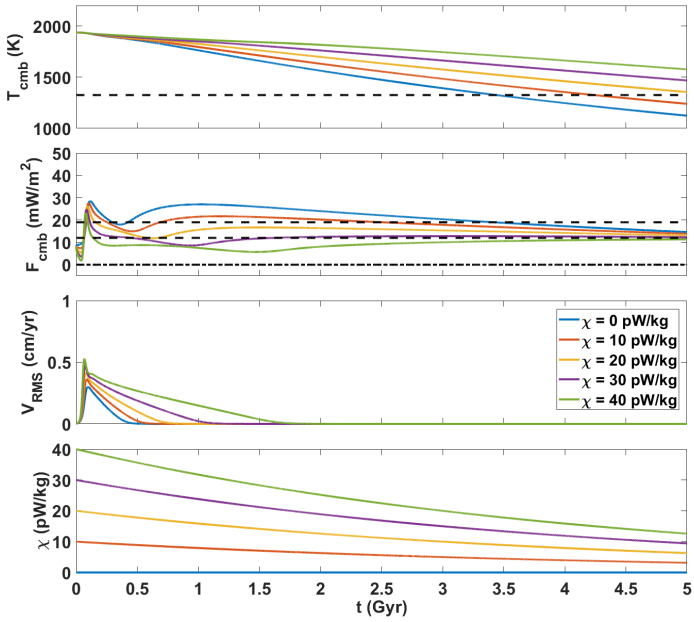

Figure 1. Time series are plotted for CMB temperature (first panel), basal heat flux (second panel), V_{RMS} (third panel), and mantle internal heating rate (fourth panel) for five calculations with different initial internal heat production rates (indicated in the legend) and κ = 2 mm^2/s. In the first panel, the dashed black line represents the solidus temperature of the core, T = 1325 K, evaluated at the core-mantle boundary pressure assuming an Fe-S-Si mixture. In the second panel, a range of core heat flux values (12 - 19 mW/m^2) is indicated by the dashed black lines.

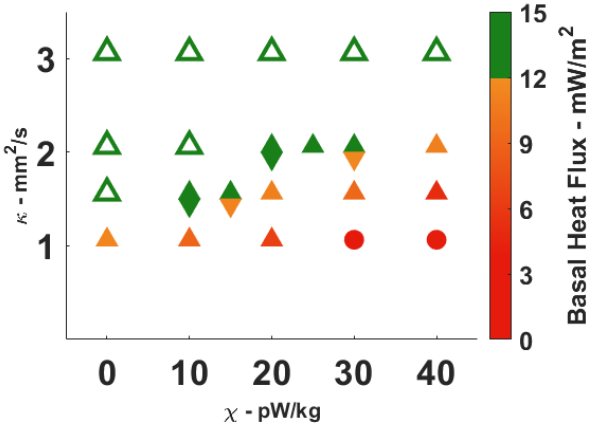

Figure 2. All calculations are summarized in χ-κ space at t = 4.5 Gyr. The basal heat flux is specified in the colorbar. An open symbol represents cases where the core-mantle boundary temperature has decreased below the solidus temperature (i.e., a solid core). A solid symbol represents cases where the core temperature exceeds the solidus. Calculations that have reached a conductive state are indicated by triangles and those that have remained convective are indicated by circles. Upward pointing triangles indicate cases where the reference viscosity is 1.0×10^{21} Pa.s and downward pointing triangles indicate cases with a reference viscosity of 0.2×10^{21} Pa.s.

References: [1] Margot, J. L., Peale, S. J., Jurgens, R. F., Slade, M. A., & Holin, I. V. (2007). Science, 316(5825), 710-714.[2] Anderson, B. J., Johnson, C. L., Korth, H., Purucker, M. E., Winslow, R. M., Slavin, J. A., ... & Zurbuchen, T. H. (2011). Science, 333(6051), 1859-1862. [3] Anderson, B. J., Johnson, C. L., Korth, H., Winslow, R. M., Borovsky, J. E., Purucker, M. E., ... & McNutt, R. L. (2012). JGR: Planets, 117(E12). [4] Cao, H., Aurnou, J. M., Wicht, J., Dietrich, W., Soderlund, K. M., & Russell, C. T. (2014). GRL, 41(12), 4127-4134. [5] Tosi, N., Grott, M., Plesa, A. C., & Breuer, D. (2013). JGR: Planets, 118(12), 2474-2487. [6] Michel, N. C., Hauck, S. A., Solomon, S. C., Phillips, R. J., Roberts, J. H., & Zuber, M. T. (2013). JGR: Planets, 118(5), 1033-1044. [7] Thiriet, M., Breuer, D., Michaut, C., & Plesa, A. C. (2019). PEPI, 286, 138-153. [8] Tackley, P. J. (2008). PEPI, 171(1), 7-18. JGR, 90, 1151–1154. [9] Yao, C., Deschamps, F., Lowman, J. P., Sanchez-Valle, C., & Tackley, P. J. (2014). JGR: Planets, 119(8), 1895-1913. [10] Hauck, S., Grott, M., Byrne, P. K., Denevi, B., Stanley, S., & McCoy, T. (2018). Mercury's global evolution. [11] Hauck II, S. A., Dombard, A. J., Phillips, R. J., & Solomon, S. C. (2004). EPSL, 222(3-4), 713-728.